*Inorg. Chem.* **2008**, *47*, 4215−4225

# Three New Cu−Azido Polymers and Their Systematic Interconversion: Role of the Amount of the Blocking Amine on the Structural Diversity and Magnetic Behavior

**Kartik Chandra Mondal and Partha Sarathi Mukherjee***

*Department of Inorganic and Physical Chemistry, Indian Institute of Science, Bangalore-560012, India*

Received November 13, 2007

Three new coordination polymers $[Cu_5(N_3)_{10}(en)_2]_n$ (**1**), $[Cu_6(N_3)_{12}(en)_4]_n$ (**2**), and $[Cu_4(N_3)_8(en)_4]_n$ (**3**) have been synthesized in a controlled manner by treatment of a 1:2 mixture of $Cu(NO_3)_2$ and $NaN_3$ with varying amount of ethylenediamine (en). Single-crystal structure analyses clearly indicated that the puckered $Cu_4$ biscubane unit in **1** gradually opens to a slightly more open $Cu_4$ macrocyclic unit in **2** when more en approaches to the $Cu_4$ core. Upon addition of further en, an open $Cu_4$ linear secondary building unit was obtained in complex **3**. Complex **1** contains four different kinds of bridging modes of the azide anion and is a complicated 3D polymer. Similarly, complexes **2** and **3** are 3D and 2D polymers, respectively, containing three different kinds of bridging azides. Complex **3** contains two very rare cis end-to-end (EE) and single-end-on (EO) azido modes. Structural transformation from **1** to **3** was monitored and explained qualitatively. Variable-temperature magnetic studies in the temperature range of 300−2 K reveal the existence of dominant ferromagnetic behavior in all the three cases with a metamagnetic-type behavior in complex **1** with the critical field of transition at 0.8 T. The purity of all the complexes were established by elemental analyses, as well as by the powder XRD patterns that matched well with the expected patterns from the single-crystal structure analysis.

## Introduction

In the past two decades, chemists and physicists have dedicated their efforts to the study of magnetic materials with the need to understand the fundamental science associated with magnetic interactions between the paramagnetic centers and the bridging ligand, enabling the design and synthesis of interesting magnetic materials.[1] These magnetic materials can be constructed to yield discrete assemblies to extended structures,[1,2] with the paramagnetic metal ions using bridging ligands that act as a superexchange pathway between the metal centers. This superexchange pathway determines the nature and magnitude of the exchange coupling parameter *J*. In many cases, either azido or carboxylate moieties have been used as bridging ligands because of their versatile bridging modes (Scheme 1). In general, the very common bridging modes observed for the azido linker are end-to-end (EE) and end-on (EO). The former one is mainly known as antiferromagnetic coupler (AF) with a few exceptions where ferromagnetic interaction through this pathway was also observed.[1n,3a] The EO mode can mediate both ferro- and antiferromagnetic interactions depending on the Cu−N−Cu bond angle. For the $Cu^{II}$ system, it is observed that when this angle is less than 108°, the complex shows ferromagnetic properties, and when it is larger than 108°, the magnetic interaction between the paramagnetic centers is antiferromagnetic in nature.[3,10c] In a majority of the cases, the investigations of metal−azido systems have been mainly focused on the low dimensionalities.[4,5] High-dimensional networks of metal−azido derivatives are of particular interest because of their novel topology and enhancement of bulk magnetic properties, as well as their magnetostructural correlations. The most common strategy employed for the synthesis of a high-dimensional metal−azido system is the further extension of metal−azido assemblies, using neutral organic linkers with a few recent examples where ionic organic linkers have also been used for this purpose.[6] Alternatively, the use of more azido anion by addition of a countercation, such as $N(CH_3)_4^+$ has also been established.[7] The denticity of the blocking amine ligand has strong influence on the bridging mode of the azido ligand and the dimensionality of polynuclear metal−azido systems. Higher

* To whom correspondence should be addressed. E-mail: psm@ipc.iisc.ernet.in. Fax: 91-80-23601552. Phone: 91-80-22933352.

10.1021/ic702232d CCC: $40.75 
Published on Web 04/17/2008

denticity of the blocking chelating ligand reduces the available sites on the metal for coordination and thus favors low dimensionality. It has been also found from the literature that a simple change in the substitution on the amine ligand dramatically changes the structure and magnetic behavior of the metal−azido systems.[6] The change in the amount of the blocking amine ligand should in principle change the structural pattern of azido−metal systems. This prompted us to see the effect of systematic change in the amount of the blocking amine on the structural change on the Cu−azido system. Here we report the synthesis, structural characterization, and variable-temperature magnetic behavior of three new Cu−azido polymers $[Cu_5(N_3)_{10}(en)_2]_n$ (**1**), $[Cu_6(N_3)_{12}(en)_4]_n$ (**2**), and $[Cu_4(N_3)_8(en)_4]_n$ (**3**) [en = ethylenediamine]. The complexes were synthesized by simply varying the amount of blocking ethylenediamine (en) per copper unit. Structural characterizations reveal that the first two polymers are 3D, while the third one is a 2D sheet. This represents the first report on the structural diversity of metal−azido systems by systematic varying the amount of blocking amine ligand. Complex **1** contains 1,1; 1,3; 1,1,1; as well as 1,1,3, bridging azides, representing the first example of a metal−azido system containing four different modes of azido linker. Most interestingly, the transformation of complex **1** to complex **3** via the intermediate **2** has been monitored in mother liquor.

## Experimental Section

**Materials.** $Cu(NO_3)_2 \cdot 3H_2O$, $NH_4HF_2$, $NaN_3$, and ethylenediamine (en) were obtained from commercial sources and were used as received without further purification.

**Physical Measurements.** Elemental analyses of C, H, and N were performed using a Perkin-Elmer 240C elemental analyzer. IR spectra were recorded as KBr pellets using a Magna 750 FT-IR spectrophotometer. The measurements of variable-temperature magnetic susceptibility and field dependence of magnetization were carried out on a Quantum Design MPMS-XL5 SQUID magnetometer. Susceptibility data were collected using an external magnetic field of 0.2 T for **1** and **3** and at 0.5 T for **2** in the temperature range of 2 to 300 K. The experimental susceptibilities were corrected for diamagnetism (Pascal's tables).[8]

***Caution!*** *Azido complexes of metal ions in the presence of organic ligands are potentially explosive. Only a small amount of material should be prepared, and it should be handled with care.*

**Synthesis of the Complex $[Cu_5(N_3)_{10}(en)_2]_n$ (1).** To a 7 mL methanolic solution of $Cu(NO_3)_2 \cdot 3H_2O$ (1.00 mmol, 187 mg) and en (1.00 mmol, 60 mg), a mixture of $H_4NHF_2$ (1.00 mmol; 53 mg) and $NaN_3$ (1.00 mmol; 65 mg) in minimum water was added slowly. The mixture was heated at 50 °C for a few minutes and filtered. Thin plate-shaped crystals of **1** were obtained in 12 h. $H_4NHF_2$ was added as a buffer. It was assumed that because it is a source of ammonium ions, $H_4NHF_2$ may protonate en to some extent, and thus availability of free en in the solution will reduce. Isolated Yield:


(1) (a) Kahn, O. *Chem. Phys. Lett.* **1997**, *265*, 165. (b) Aubin, S. M. J.; Bolcar, M. A.; Christou, G.; Eppley, H. J.; Folting, K.; Hendrickson, D. N.; Huffman, J. C.; Squire, R. C.; Tsai, H. L.; Wang, S.; Wemple, M. W. *Polyhedron* **1998**, *17*, 3005. (c) Thomas, L.; Lionti, F.; Ballou, R.; Gatteschi, D.; Sessoli, R.; Barbara, B. *Nature* **1996**, *383*, 145. (d) *Magnetic Molecular Materials*; Gatteschi, D., Kahn, O., Miller, J. S., Palacio, F., Eds.; Kluwer Academic: Dordrecht, The Netherlands, 1991. (e) Stamatatos, T. C.; Christou, A. G.; Jones, C. M.; O'Callaghan, B. J.; Abboud, K. A.; O'Brien, T. A.; Christou, G. *J. Am. Chem. Soc.* **2007**, *129*, 9840. (f) Bagai, R.; Abboud, K. A.; Christou, G. *Inorg. Chem.* **2007**, *46*, 5567. (g) Sessoli, R.; Tsai, H-L.; Schake, A. R.; Wang, S.; Vincent, J. B.; Folting, K.; Gatteschi, D.; Christou, G.; Hendrickson, D. N. *J. Am. Chem. Soc.* **1993**, *115*, 1804. (h) Ouellette, W.; Galan-Mascaros, J. R.; Dunbar, K. R.; Jubieta, J. *Inorg. Chem.* **2006**, *45*, 1909. (i) Shatruk, M.; Dragulescu, A. A.; Chambers, K. E.; Stoian, S. A.; Bominaar, F. A.; Achim, C.; Dunbar, K. R. *J. Am. Chem. Soc.* **2007**, *129*, 6104. (j) Konar, S.; Zangrando, E.; Drew, M. G. B.; Mallah, T.; Ribas, J.; Ray Chaudhuri, N. *Inorg. Chem.* **2003**, *42*, 5966. (k) Tabellion, F. M.; Seidel, S. R.; Arif, A. M.; Stang, P. J. *J. Am. Chem. Soc.* **2001**, *123*, 11982. (l) Tolis, E. I.; Helliwell, M.; Langley, S.; Raftery, J.; Winpenny, R. E. P. *Angew Chem., Int. Ed.* **2003**, *42*, 3804. (m) Winpenny, R. E. P. *Dalton Trans.* **2002**, 1. (n) Ribas, J.; Escuer, A.; Monfort; Vicente, R.; Cortés, R.; Lezama, L.; Rojo, T. *Coord. Chem. Rev.* **1999**, *193*−*195*, 1027. and references therein. (o) Kato, M.; Muto, Y. *Coord. Chem. Rev.* **1988**, *92*, 45.

(2) (a) Mondal, K. C.; Song, Y.; Mukherjee, P. S. *Inorg. Chem.* **2007**, *46*, 9736. (b) Price, D. J.; Murry, K. S. *Chem. Commun.* **2002**, 762. (c) Konar, S.; Zangrando, E.; Drew, M. G. B.; Mallah, T.; Ray Chaudhuri, N. *Inorg. Chem.* **2003**, *42*, 5966. (d) Maji, T. K.; Mostafa, G.; Mallah, T.; Boquera, J. C.; Ray Chaudhuri, N. *Chem. Commun.* **2001**, 1012. (e) Sessoli, R.; Gatteschi, D.; Caneschi, A.; Novak, M. A. *Nature* **1993**, *365*, 141. (f) Wernsdorfer, W.; Aliaga-Alcalde, N.; Hendrickson, D. N.; Christou, G. *Nature* **2002**, *416*, 406. (g) Müller, A.; Meyer, J.; Krickemeyer, E.; Beugholt, C.; Bögge, H.; Peters, F.; Schmidtmann, M.; Kögerler, P.; Koop, M. J. *Chem.*−*Eur. J.* **1998**, *4*, 1000. (h) Leibeling, G.; Demeshko, S.; Bauer-Siebenlist, B.; Meyer, F.; Pritzkow, H. *Eur. J. Inorg. Chem.* **2004**, 2413. (i) Demeshko, S.; Leibeling, G.; Dechert, S.; Meyer, F. *Dalton Trans.* **2006**, 3458.

(3) (a) Mukherjee, P. S.; Maji, T. K.; Mostafa, G.; Mallah, T.; Ray Chaudhuri, N. *Inorg. Chem.* **2000**, *39*, 5147. (b) Comarmond, J.; Plumere, P.; Lehn, J. M.; Agnus, Y.; Louis, R.; Weiss, R.; Kahn, O.; Morgesten-badarau, I. *J. Am. Chem. Soc.* **1982**, *104*, 6330. (c) Kahn, O.; Sikorav, S.; Gouteron, J.; Jeannin, S.; Jeannin, Y. *Inorg. Chem.* **1983**, *22*, 2877. (d) Tandon, S. S.; Thompson, L. K.; Manuel, M. E.; Bridson, J. N. *Inorg. Chem.* **1994**, *33*, 5555. (e) Ribas, J.; Monfort, M.; Ghosh, B. K.; Solans, X.; Font-Bardia, M. *J. Chem. Soc., Chem. Commun.* **1995**, 2375. (f) Ribas, J.; Monfort, M.; Ghosh, B. K.; Solans, X. *Angew. Chem., Int. Ed. Engl.* **1994**, *33*, 2177. (g) Viau, G.; Lambardi, G. M.; De Munno, G.; Julve, M.; Lloret, F.; Faus, J.; Caneschi, A.; Clemente-Juan, J. M. *Chem. Commun.* **1997**, 1195. (h) Escuer, A.; Vicente, R.; Ribas, J.; El Fallah, M. S.; Solans, X.; Font-Bardia, M. *Inorg. Chem.* **1993**, *32*, 3727. (i) Ruiz, E.; Cano, J.; Alvarez, S.; Alemany, P. *J. Am. Chem. Soc.* **1998**, *120*, 11122. (j) Aebersold, M. A.; Gillon, M.; Plantevin, O.; Pardi, L.; Kahn, O.; Bergerat, I.; Seggern, V.; Ohrstrom, L.; Grand, A.; Lelievre-Berna, E. *J. Am. Chem. Soc.* **1998**, *120*, 5238.

(4) (a) Abu-Youssef, M. A. M.; Escuer, A.; Goher, M. A. S.; Mautner, F. A.; Reib, G. J.; Vicente, R. *Angew. Chem., Int. Ed.* **2000**, *39*, 1624. (b) Liu, X.-T.; Wang, X.-Y.; Zhang, W.-X.; Cui, P.; Gao, S. *Adv. Mater.* **2006**, *18*, 2852. (c) Liu, T.-F.; Fu, D.; Gao, S.; Zhang, Y.-Z.; Sun, H. L.; Su, G.; Liu, Y.-J. *J. Am. Chem. Soc.* **2003**, *125*, 13976. (d) Hong, C. S.; Koo, J.-E.; Son, S.-K.; Lee, Y. S.; Kimand, Y.-S.; Do, Y. *Chem.*−*Eur. J.* **2001**, *7*, 4243. (e) Ko, H. H.; Lim, J. H.; Kim, H. C.; Hong, C. S. *Inorg. Chem.* **2006**, *45*, 8847. (f) Escuer, A.; Goher, M. A. S.; Mautner, F. A.; Vicente, R. *Inorg. Chem.* **2000**, *39*, 2107. (g) Escuer, A.; Vicente, R.; El, M. S.; Fallah, M. A.; Goher, S.; Mautner, F. A. *Inorg. Chem.* **1998**, *37*, 4466. (h) Das, A.; Rosair, G. M.; Fallah, M. S.; El Ribas, J.; Mitra, S. *Inorg. Chem.* **2006**, *45*, 3301.

(5) (a) Shen, Z.; Zuo, J.-L.; Gao, S.; Song, Y.; Che, C.-M.; Fu, H.-K.; You, X.-Z. *Angew. Chem., Int. Ed.* **2000**, *39*, 3633. (b) Monfort, M.; Resino, I.; Ribas, J.; Stoeckli-Evans, H. *Angew. Chem., Int. Ed.* **2000**, *39*, 191. (c) Gao, E.-Q.; Yue, Y.-F.; Bai, S.-Q.; He, Z.; Yan, C.-H. *J. Am. Chem. Soc.* **2004**, *126*, 1419. (d) You, Y. S.; Yoon, J. H.; Kim, H. C.; Hong, C. S. *Chem. Commun.* **2005**, 4116. (e) He, Z.; Wang, Z.-M.; Gao, S.; Yan, C.-H. *Inorg. Chem.* **2006**, *45*, 6694.

(6) (a) Liu, F.-C.; Zeng, Y.-F.; Li, J. R.; Bu, X.-H.; Zhang, H. J.; Ribas, J. *Inorg. Chem.* **2005**, *44*, 7298. (b) Liu, F.-C.; Zeng, Y.-F.; Jiao, J.; Li, J. R.; Bu, X.-H.; Ribas, J.; Batten, S. R. *Inorg. Chem.* **2006**, *45*, 6129. (c) Liu, F.-C.; Zeng, Y.-F.; Jiao, J.; Bu, X.-H.; Ribas, J.; Batten, S. R. *Inorg. Chem.* **2006**, *45*, 2776.

(7) (a) Mautner, F. A.; Cor; es, R.; Lezama, L.; Rojo, T. *Angew. Chem., Int. Ed. Engl.* **1996**, *35*, 78. (b) Goher, M. A. S.; Cano, J.; Journaux, Y.; Abu-Youssef, M. A.M.; Mautner, F. A.; Escuer, A.; Vicente, R. *Chem.*−*Eur. J.* **2000**, *6*, 778.

(8) (a) Dutta, R. L.; Syamal, A. *Elements of Magnetochemistry*, 2nd ed.; East West Press: Manhattan Beach, CA, 1993. (b) Kahn, O. *Molecular Magnetism*, 1993, VCH publisher.

**Scheme 1.** Different Bridging Modes of Azide and Carboxylate Anions

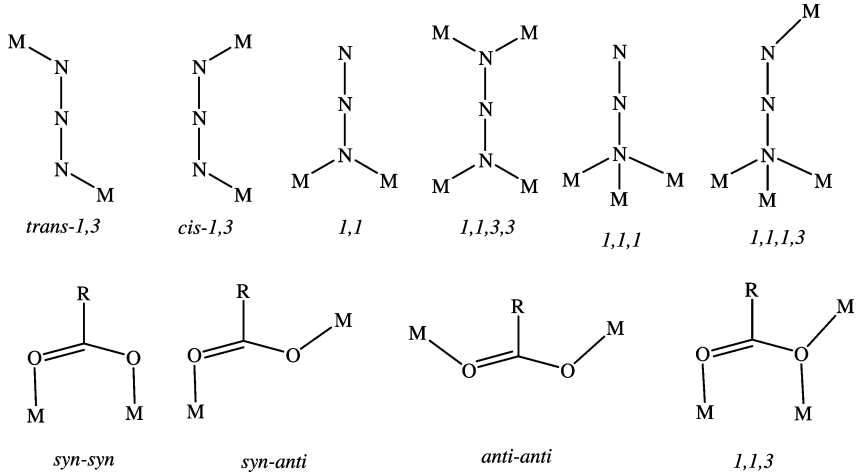


75%. Anal. Calcd for **1**, $Cu_5H_{16}C_4N_{34}$: C, 5.59; N, 55.51; H, 1.86. Found: C, 5.30; N, 55.25; H, 1.82. IR bands ($cm^{-1}$): 3332, 3305, 3250, 2102, 2082, 2055, 2037.

The same complex was also prepared in a different way: To the methanolic solution (5 mL) of $Cu(NO_3)_2 \cdot 3H_2O$ (1.25 mmol; 235 mg) and ethylenediamine (0.25 mmol, 15.0 mg), an aqueous solution (2 mL) of $NaN_3$ (2.50 mmol, 162 mg) was added to produce a gray-brown precipitate, which was stirred for five minutes. A dark gray-brown precipitate containing the reaction mixture and $Cu^{II}$−azido was obtained in a few seconds. The resulting mixture was stirred for 15 min at 60 °C and filtered hot. Dark gray plate-shaped crystals of **1** were obtained (isolated yield = 60%) from the filtrate in 12 h. Following this method, crystals of the three compounds can be subsequently obtained if individual complexes are not separated from the mother liquor.

**Synthesis of the Complex $[Cu_6(N_3)_{12}(en)_4]_n$ (2).** To a methanolic solution (5 mL) of $Cu(NO_3)_2 \cdot 3H_2O$ (1.00 mmol, 187 mg) and ethylenediamine (0.66 mmol, 40 mg), an aqueous solution of $NaN_3$ (2.00 mmol; 130 mg) was added without stirring to get a dark green solution from which rod-shaped crystals of complex $[Cu_6(N_3)_{12}(en)_4]_n$ (**2**) were obtained after 2 days. The isolated yield was 86%. Anal. Calcd for **2**, $Cu_6H_{32}C_8N_{44}$: C, 8.53; N, 54.75; H, 2.84. Found: C, 8.30; N, 54.62; H, 2.66. IR bands ($cm^{-1}$): 3326, 3240, 2946, 2099, 2079, 2056, 2036.

**Synthesis of the Complex $[Cu_4(N_3)_8(en)_4]_n$ (3).** Large hexagonal crystals of complex **3** were obtained in 75% yield after 6 days when the rod-shaped crystals of complex **2** were not separated from the above reaction mixture (synthesis of complex **2**). The yield of the complex **3** was improved by application of the following synthetic procedure.

To a methanolic solution (7 mL) of $Cu(NO_3)_2 \cdot 3H_2O$ (2.00 mmol, 376 mg) an aqueous solution of $NaN_3$ (2.00 mmol, 130 mg) was added without stirring to get an immediate brown slurry, into which ethylenediamine (2 mmol; 130 mg) was added, and the mixture was left for 10 days to obtain exclusively hexagonal crystals of complex **3** in 88% yield. Anal. Calcd for **3**, $Cu_4H_{32}C_8N_{32}$: C, 11.56; N, 53.97; H, 3.85. Found: C, 11.25; N, 53.70; H, 3.92. IR bands ($cm^{-1}$): 3324, 3291, 3145, 2966, 2092, 2070, 2059, 2031.

**Crystal Structure Determinations.** X-ray single-crystal data for **1**, **2**, and **3** were collected using a Bruker SMART APEX CCD diffractometer, equipped with a fine-focus sealed-tube Mo Kα X-ray source. The SMART program was used for data acquisition, and the SAINT program was used for data extraction. The structures were solved using direct methods with the SHELX-97 program.[9] The non-hydrogen atoms were refined with anisotropic thermal parameters. The disordered atoms were refined with constrained dimensions. The hydrogen atoms bonded to carbon were included in geometric positions and given thermal parameters equivalent to 1.2 times those of the atom to which they were attached. An absorption correction was carried out using the ABSPACK program. Crystallographic data and refinement parameters are given in Table 1.

**Table 1.** Crystal Data and Structure Refinement Parameters for Compounds **1**, **2**, and **3**

| compound | **1** | **2** | **3** |
|---|---|---|---|
| empirical formula | $Cu_5H_{16}C_4N_{34}$ | $Cu_6H_{32}C_8N_{44}$ | $Cu_4H_{32}C_8N_{32}$ |
| fw | 857.5 | 1125 | 830 |
| $T$ (K) | 293(2) | 293(2) | 293(2) |
| space group | $P\bar{1}$ | $P2_1/n$ | $C2/c$ |
| $a$ (Å) | 6.8758(16) | 8.186(5) | 17.699(7) |
| $b$ (Å) | 8.460(2) | 14.187(8) | 6.411(2) |
| $c$ (Å) | 12.115(3) | 16.577(10) | 26.250(10) |
| α (deg) | 96.690(4) | 90.00 | 90.00 |
| $\beta$ (deg) | 92.487(4) | 98.196(10) | 100.037(6) |
| $\gamma$ (deg)°= | 107.104(4) | 90.00 | 90.00 |
| $V$ ($Å^3$) | 666.8(3) | 1906(2) | 2932.8(18) |
| $Z$ | 2 | 4 | 8 |
| $\mu$(Mo Kα) ($mm^{-1}$) | 3.990 | 3.364 | 2.297 |
| $\lambda$ (Å) | 0.71073 | 0.71073 | 0.71073 |
| $R_w{}^a$ | 0.2488 | 0.1521 | 0.0855 |
| $R^a$ | 0.0742 | 0.0621 | 0.0367 |
| $D$ (Mg $m^{-3}$) | 1.454 | 1.517 | 1.882 |

$^a R = \sum||F_o| - |F_c||/\sum|F_o|$; $R_w = [\sum\{w(F_o^2 - F_c^2)^2\}/\sum\{w(F_o^2)^2\}]^{1/2}$.

## Results and Discussion

**Synthesis.** Complex **1** was obtained by using 0.2 equiv of en with $Cu^{II}$ in presence of azide. If the same reaction is performed in presence of a higher amount of en (0.66 equiv), plate-shaped crystals of complex **2** were formed in two days. Interestingly, when the same reaction was performed using 2 equiv of azide, followed by 1 equiv of en (synthesis of **3**), thin plates of complex **1** were formed in 10−12 h. These thin plates of **1** dissolved in the mother liquor and slowly transformed exclusively to rod-shaped crystals of complex **2** in two days. Finally, hexagonal crystals of complex **3** were obtained when the same reaction mixture was allowed to stay at ambient temperature for 6 days. This observation

(9) (a) Sheldrick, G. M. *SHELXL-97*; University of Göttingen: Göttingen, Germany, 1997. (b) Sluis, P. V.D.; Spek, A. L. *Acta Crystallogr.* **1990**, *A46*, 194.

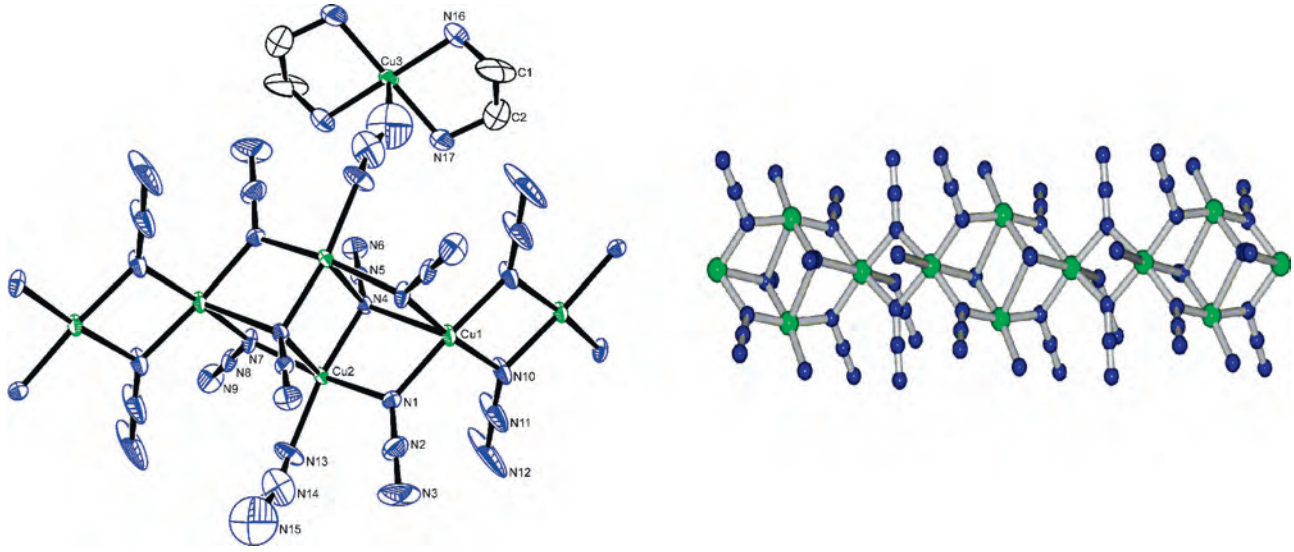


**Figure 1.** ORTEP view of the main unit of **1** with atom numbering scheme (left). The view of the 1D rail-road unit in complex **1** (right).

suggests that complex **1** slowly transforms to **3** via the intermediate **2**. However, this conversion was not observed if the individual complexes are separated from the mother liquor. Complexes **1**−**3** were also synthesized in higher yield by varying the amount of ethylenediamine as mentioned in the Experimental Section. The purity and identity of each phase were established very well by the elemental analyses, as well as from the powder XRD patterns of the complexes, which matched well with the expected patterns from the single crystal structures (see Supporting Information).

The IR ($cm^{-1}$) spectra of the complexes showed absorption peaks in the range of 3332−2946 $cm^{-1}$ which are assigned to $\nu_{as}$(N−H) of the ethylenediamine. Peaks in the range of 2102−2036 $cm^{-1}$ are the result of the presence bridging azido anions. Multiple peaks in all the three cases are indicative of multiple bridging modes of the azido.

**Structure Description of $[Cu_5(N_3)_{10}(en)_2]_n$ (1).** The structure determination of complex **1** reveals that it is complicated 3D polymer. The basic secondary building unit in the polymer is a $Cu_4$ incomplete dicubane cluster (Figure 1). The tetranuclear $Cu_4N_6$ can be viewed as two face-sharing $Cu_3N_4$ cubane units with one copper site being vacant. The crystallographic asymmetric unit of **1** consists of two and half $Cu^{II}$, one ethylenediamine, and five azides for its charge balance, and hence there are three crystallographically distinct $Cu^{II}$ ions present.

The basic secondary building unit consists of two $\mu_{1,1,1}$-azido [Cu(2)−N(4) = 1.990 Å, Cu(2*)−N(4) = 2.554 Å, Cu(1)−N(4) = 2.505 Å,] anions, two $\mu_{1,1}$-azido [Cu(1)−N(1) = 1.976 Å and Cu(2)−N(1) = 2.015 Å] and two $\mu_{1,1,3}$-azido [Cu(2)−N(7) = 2.016 Å, Cu(1)−N(7) = 2.007 Å, and Cu(1*)−N(9) = 2.708 Å] to form a defective dicubane $Cu_4N_6$ core that is connected further by two $\mu_{1,1}$-azido anions [Cu(1)−N(10) = 1.993Å and Cu(1*)−N(10) = 1.982 Å] to form a rail-road type 1D core (Figure 1). This 1D rail road unit in the complex is further linked to neighboring chains via $Cu(en)_2(N_3)$ units via a 1,3-bridging azido fashion to form a 2D corrugated net (Figure-2). Neighboring 2D sheets are further linked by $\mu_{1,1,3}$-azido linkers to form a complicated 3D polymer (Figure 2). Thus the final three-dimensional assembly contains four different kinds of bridging azido (1,3; 1,1; 1,1,3 and 1,1,1,3). To the best of our knowledge this represents the first example of a Cu-azido system containing four different kind azido bridging modes. The shortest interchain Cu−Cu distance in the 2D sheet through the $Cu(en)_2(N_3)_2$ moiety is 12.55 (8) Å, while the shortest inter sheet Cu−Cu distance through the 1,1,3-bridging azido pathway is 5.55(7) Å. Selected bond parameters around the $Cu^{II}$ in this complex are provided in Table 2.

**Crystal Structure of Complex $[Cu_6(N_3)_{12}(en)_4]_n$ (2).** The crystallographic asymmetric unit of this complex consists of three $Cu^{II}$, two ethylenediamine, and six azido anions for charge balance. Cu(1) and Cu(2) are coordinated by one $\mu_{1,1}$-azido and one $\mu_{1,1,3}$-azido anion to form a dimeric unit that is connected by $\mu_{1,1,3}$-azido anion to $Cu(en)_2^{2+}$ cation to afford a trimeric unit (Figure 3). Two different kinds of 1,1,3-azido bridging modes are present in this complex. In one case, one terminal nitrogen links to the axial site of a $Cu_2$ dimeric unit and the axial site of a $Cu(en)_2^{2+}$moiety. The second 1,1,3-bridging azido linking two $Cu^{II}$ ions of the dimeric unit through one terminal nitrogen and other terminal nitrogen links the axial site of the $Cu(en)_2^{2+}$moiety. The Cu−N−Cu bond angle formed by the first kind of 1,1,3-azido is 126°, while the second 1,1,3-azido creates a 102 °Cu−N−Cu bond angle. The first kind of 1,1,3-azido anions link two $Cu_2$ dimers to form a $Cu_4$ basic unit (Figure-3). The repeating $Cu_4$ secondary building unit composed of four $Cu^{II}$ and eight azido anions. Cu(1) and Cu(2) of the dimeric unit are in square-planar and square-pyramidal geometries, respectively. Cu(3) is in octahedral environment with the equatorial sites occupied by the chelating en ligands and the axial sites are coordinated to two 1,1,3-bridging azido. The crystal structure reveals a weak interaction Cu(2)−N(1) of 2.783 Å through the axial site. The tetrameric unit has been repeated by the $Cu(en)_2(N_3)_2$ units through the azide linkers to result the final 3D complicated structure (Figure 3). Selected bond parameters are assembled in Table-2. The Cu−Cu distance within the $Cu_2$ dimeric unit is 3.134(6) Å.

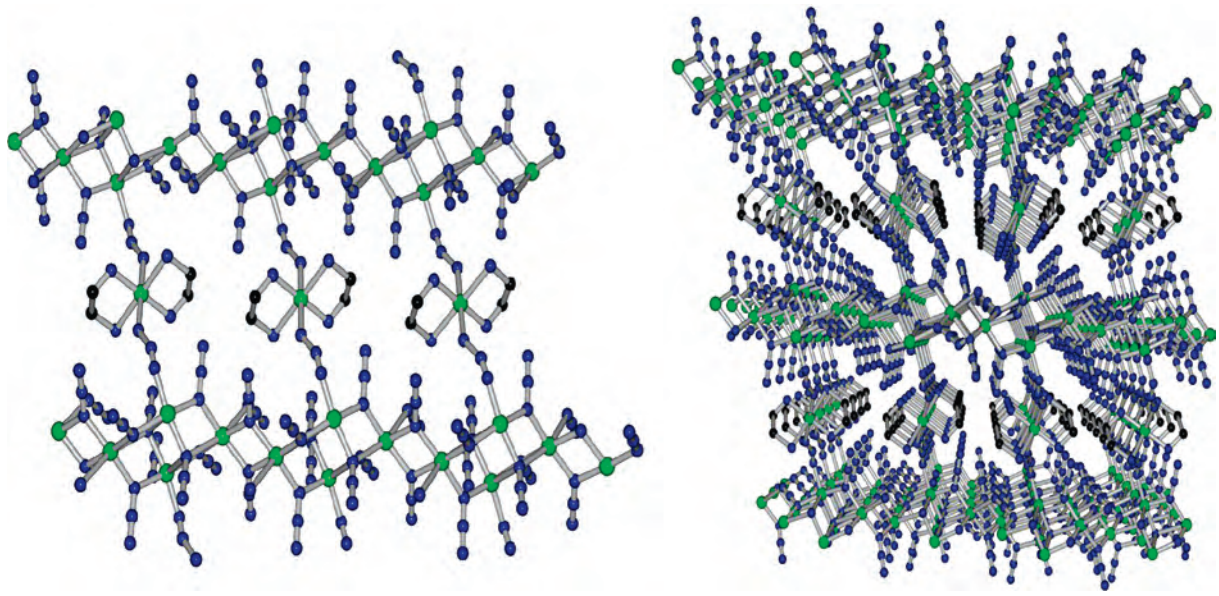

**Figure 2.** View of the 2D sheet (left) unit in **1** and the final 3D network along crystallographic *a* axis (right).

**Crystal Structure of Complex $[Cu_4(N_3)_8(en)_4]_n$ (3).** The crystallographic asymmetric unit of the complex **3** consists of two $Cu^{II}$, two ethylenediamine, and four azido ions. The coordination environment around one copper is octahedral, while the other one is square-pyramidal. In contrast to the earlier two complexes, each $Cu^{II}$ of this complex is coordinated to one chelating en ligand. The $Cu^{II}$ ions of the asymmetric unit are linked by a very rare single end-on azido linker.[3a] Single end-to-end azido bridging is quite common,[3] but whenever an azide bridges two metals in end-on fashion, it is always associated with a second azide or another bridging moiety ($OH^-$ or $COO^-$ etc.).[10] In an earlier report, we first reported the possibility of this kind of bridging.[3a] Because of the presence of a single azido anion between two metal centers, single end-on azido bridge generally allows a large M−N−M angle separation (≥120°). Surprisingly, in complex **3**, this angle is 98.98°, which represents the shortest M−N−M bond angle for a single end-on azido bridge reported so far. Two adjacent asymmetric dimeric units are linked further by double end-on azido linkers to form the basic repeating $Cu_4$ secondary building unit of this complex (Figure 4).

The end-to-end azido linker always links the metal centers in the most favorable trans fashion with a single exception,[11] where it showed a cis-type of coordination. The end-to-end azido linker links the adjacent repeating basic $Cu_4$ building units in complex **3** in an unusual cis conformation to result a 1D chain motif. The neighboring chains are further linked by the cis-EE azido linkers through the crystallographic *b* axis to result the final 2D sheet structure (Figure-5). The most surprising aspects in this complex are the presence of two rare kinds of azido bridging modes (single EO and cis-EE) and the larger Cu−N−Cu (100.39°) bond angle through the double EO azido pathway than the angle through single EO azido pathway (98.98°), even though the reverse order is expected. The Cu−Cu distances through the double and single EO azido pathways are 3.655 and 3.498 Å, respectively.

**Structural Correlation.** Complex **1** is the parent member of this three Cu−azido−en complexes series. The parent transforms to **3** via the intermediate **2** in presence of more chelating ligand en with time. This observation can be qualitatively supported by the crystal packing nature. In complex **1**, the main secondary building unit is a defective biscubane $Cu_4N_6$ unit, which extends to a 1D rail-road fashion. The $Cu_4(N_3)_8$ biscubane cluster does not contains any en ligand. Each $Cu_4$ cluster connects to a $Cu(en)_2(N_3)_2$ counter unit to extend the network. With a slight increase in the amount of the en, one more $Cu(en)_2(N_3)_2$ approaches per $Cu_4$ cluster unit. This approach results in the breaking of a Cu−N between the Cu and 1,1,1-azido resulting in the formation of a more open, but still closed, $Cu_4$ building unit in **2**. Upon further increase in the amount of en per copper, each $Cu^{II}$ coordinates to one en ligand, which helps the cyclic $Cu_4$ secondary building unit to open up to a more open linear $Cu_4$ repeating unit in complex **3**. We think that at first more-puckered Cu−azide core was formed for the fulfillment of all the coordination sites of $Cu^{II}$ centers and then that puckered Cu−azido core was approached by en to give the

(10) (a) Tandon, S. S.; Thompson, L. K.; Miller, D. O. *J. Chem. Soc., Chem. Commun.* **1995**, 1907. (b) Mautner, F. A.; Hanna, S.; Cortés, R.; Lezema, L.; Gotzone, M.; Rojo, T. *Inorg. Chem.* **1999**, *38*, 4647. (c) Tandon, S. S.; Thompson, L. K.; Manuel, M. E.; Bridson, J. N. *Inorg. Chem.* **1994**, *33*, 5555. (d) Escuer, A.; Vicente, R.;.; Ribas, J. M. S.; El Fallah, M. S.; Solans, X. *Inorg. Chem.* **1993**, *32*, 1033. (e) Ribas, J.; Monfort, M.; Diaz, C.; Bastos, C.; Solans, X. *Inorg. Chem.* **1994**, *33*, 484. (f) Escuer, A.; Vicente, R.; Ribas, J.; El Fallah, M. S.; Solans, X.; Font-Bardía, M. *Inorg. Chem.* **1994**, *33*, 1842. (g) Vicente, R.; Escuer, A.; Ribas, J.; El Fallah, M. S.; Solans, X.; Font-Bardía, M. *Inorg. Chem.* **1995**, *34*, 1278. (h) Ribas, J.; Monfort, M.; Ghosh, B. K.; Cortés, R.; Solans, X.; Font-Bardía, M. *Inorg. Chem.* **1996**, *35*, 864. (i) Abersold, M. A.; Gillon, B.; Plantevin, O.; Pardi, L.; Kahn, O.; Bergerat, P.; Seggern, I.; Tuczek, F.; Öhrström, L.; Grand, A.; Ávre-Berna, E. *J. Am. Chem. Soc.* **1998**, *120*, 5238.

(11) (a) Hong, C. S.; Koo, J.; Son, S. K.; Lee, Y. S.; Kim, Y. S.; Do, Y. *Chem.—Eur. J.* **2001**, *7*, 4243. (b) Zeng, Y. F.; Jhao, J. P.; Hu, B. W.; Hu, X.; Liu, F. C.; Ribas, J.; Arino, J. R.; Bu, X. H. *Chem.—Eur. J.* **2007**, *13*, 9924.

**Table 2.** Selected Bond Lengths (Å) and Angles (deg°) for Compounds **1**, **2**, and **3**[a]

| | | | | | |
|---|---|---|---|---|---|
| | | | **1** | | |
| Cu(1)−N(1) | 1.976(7) | Cu(1)−N(10) | 1.982(7) | Cu(1)−N(10)$^{i}$ | 1.993(7) |
| Cu(1)−N(7)$^{ii}$ | 2.007(6) | Cu(2)−N(13) | 1.967(8) | Cu(2)−N(4) | 1.990(6) |
| Cu(2)−N(7) | 2.016(7) | Cu(2)−N(1) | 2.015(7) | Cu(3)−N(16) | 1.997(8) |
| Cu(3)−N(17) | 2.41(4) | Cu(3)−N(15) | 2.23(2) | N(1)−N(2) | 1.196(10) |
| N(4)−N(5) | 1.207(9) | N(7)−N(8) | 1.203(10) | N(8)−N(9) | 1.158(10) |
| N(6)−N(5) | 1.147(9) | N(2)−N(3) | 1.127(13) | N(16)−C(1) | 1.389(19) |
| N(10)−N(11) | 1.167(12) | N(13)−N(14)$^{ii}$ | 1.149(17) | N(11)−N(12) | 1.119(15) |
| N(14)−N(15)$^{iv}$ | 1.62(4) | | | | |
| N(13)−Cu(2)−N(4) | 169.9(4) | | N(13)−Cu(2)−N(7) | | 94.4(4) |
| N(4)−Cu(2)−N(7) | 92.8(3) | | N(13)−Cu(2)−N(1) | | 91.8(3) |
| N(4)−Cu(2)−N(1) | 82.6(3) | | N(7)−Cu(2)−N(1) | | 167.2(3) |
| N(10)−Cu(1)−N(1) | 170.1(3) | | N(10)−Cu(1)−N(10)$^{i}$ | | 78.1(3) |
| N(1)−Cu(1)−N(10)$^{i}$ | 92.7(3) | | N(10)−Cu(1)−N(7)$^{ii}$ | | 97.0(3) |
| N(1)−Cu(1)−N(7)$^{ii}$ | 92.4(3) | | N(10)$^{i}$−Cu(1)−N(7)$^{ii}$ | | 173.2(3) |
| N(16)−Cu(3)−N(16)$^{iii}$ | 180.00(1) | | N(16)−Cu(3)−N(17)$^{iii}$ | | 94.7(8) |
| N(16)−Cu(3)−N(17) | 85.3(8) | | N(17)$^{iii}$−Cu(3)−N(17) | | 180.0(11) |
| N(16)−Cu(3)−N(15)$^{iii}$ | 90.5(5) | | | | |
| | | | **2** | | |
| N(12)−N(11) | 1.153(10) | Cu(1)−N(7) | 1.926(6) | Cu(1)−N(16) | 1.992(6) |
| Cu(1)−N(1) | 2.013(5) | Cu(1)−N(4) | 2.019(5) | Cu(2)−N(10) | 1.949(6) |
| Cu(2)−N(13) | 1.977(6) | Cu(2)−N(1) | 2.004(6) | Cu(2)−N(4) | 2.062(5) |
| Cu(3)−N(20) | 2.014(7) | Cu(3)−N(21) | 2.010(6) | Cu(3)−N(22) | 2.008(7) |
| Cu(3)−N(19) | 2.032(7) | N(1)−N(2) | 1.217(8) | N(11)−N(10) | 1.163(9) |
| N(2)−N(3) | 1.143(8) | N(4)−N(5) | 1.200(7) | N(5)−N(6) | 1.145(8) |
| N(8)−N(9) | 1.133(9) | N(8)−N(7) | 1.198(9) | N(20)−C(4) | 1.469(11) |
| N(14)−N(15) | 1.145(9) | N(14)−N(13) | 1.197(8) | N(19)−C(3) | 1.477(10) |
| N(22)−C(2) | 1.464(11) | N(21)−C(1) | 1.465(12) | C(4)−C(3) | 1.505(12) |
| C(1)−C(2) | 1.494(13) | N(18)−N(17) | 1.161(8) | N(17)−N(16) | 1.192(8) |
| N(7)−Cu(1)−N(16) | 92.9(3) | | N(7)−Cu(1)−N(1) | | 173.2(3) |
| N(16)−Cu(1)−N(1) | 89.6(2) | | N(7)−Cu(1)−N(4) | | 100.2(3) |
| N(16)−Cu(1)−N(4) | 164.1(2) | | N(1)−Cu(1)−N(4) | | 78.5(2) |
| N(10)−Cu(2)−N(13) | 92.3(3) | | N(10)−Cu(2)−N(1) | | 99.8(2) |
| N(13)−Cu(2)−N(1) | 167.1(2) | | N(10)−Cu(2)−N(4) | | 175.6(3) |
| N(13)−Cu(2)−N(4) | 89.9(2) | | N(1)−Cu(2)−N(4) | | 77.7(2) |
| N(20)−Cu(3)−N(21) | 95.9(3) | | N(20)−Cu(3)−N(22) | | 178.5(3) |
| N(21)−Cu(3)−N(22) | 83.4(3) | | N(20)−Cu(3)−N(19) | | 84.1(3) |
| N(21)−Cu(3)−N(19) | 177.2(3) | | N(22)−Cu(3)−N(19) | | 96.6(3) |
| Cu(2)−N(1)−Cu(1) | 102.6(2) | | N(12)−N(11)−N(10) | | 175.8(8) |
| N(3)−N(2)−N(1) | 178.1(7) | | N(11)−N(10)−Cu(2) | | 131.3(6) |
| Cu(1)−N(4)−Cu(2) | 100.4(2) | | N(6)−N(5)−N(4) | | 176.8(7) |
| N(9)−N(8)−N(7) | 175.2(9) | | N(15)−N(14)−N(13) | | 176.4(8) |
| C(2)−N(22)−Cu(3) | 111.1(5) | | N(18)−N(17)−N(16) | | 177.2(7) |
| | | | **3** | | |
| Cu(1)−N(10) | 1.994(3) | Cu(1)−N(7) | 1.999(2) | Cu(1)−N(16) | 2.021(3) |
| Cu(1)−N(15) | 2.025(3) | Cu(2)−N(4) | 1.984(3) | Cu(2)−N(13) | 1.994(3) |
| Cu(2)−N(1) | 1.996(2) | Cu(2)−N(14) | 2.009(2) | N(2)−N(3) | 1.153(3) |
| N(2)−N(1) | 1.193(3) | N(8)−N(9) | 1.142(4) | N(8)−N(7) | 1.178(3) |
| N(13)−C(3) | 1.447(4) | N(16)−C(2) | 1.465(4) | N(4)−N(5) | 1.190(4) |
| N(14)−C(4) | 1.445(4) | N(5)−N(6) | 1.144(4) | N(15)−C(1) | 1.471(4) |
| N(11)−N(12) | 1.149(3) | N(11)−N(10) | 1.195(3) | | |
| N(10)−Cu(1)−N(7) | 94.26(11) | | N(10)−Cu(1)−N(16) | | 92.77(12) |
| N(7)−Cu(1)−N(16) | 171.90(12) | | N(10)−Cu(1)−N(15) | | 175.80(11) |
| N(7)−Cu(1)−N(15) | 89.60(11) | | N(16)−Cu(1)−N(15) | | 83.50(11) |
| N(4)−Cu(2)−N(13) | 170.55(12) | | N(4)−Cu(2)−N(1) | | 95.39(11) |
| N(13)−Cu(2)−N(1) | 89.48(10) | | N(4)−Cu(2)−N(14) | | 92.65(11) |
| N(13)−Cu(2)−N(14) | 84.33(11) | | N(1)−Cu(2)−N(14) | | 165.63(11) |
| N(3)−N(2)−N(1) | 178.0(3) | | N(9)−N(8)−N(7) | | 176.8(3) |
| N(6)−N(5)−N(4) | 178.3(3) | | N(12)−N(11)−N(10) | | 177.4(3) |
| N(11)−N(10)−Cu(1) | 122.6(2) | | N(16)−C(2)−C(1) | | 109.9(3) |

[a] Symmetry transformations used to generate equivalent atoms: (i) $-x$, $-y-1$, $-z+2$; (ii) $-x$, $-y$, $-z+2$; (iii) $-x+1$, $-y$, $-z+1$; (iv) $x$, $y$, $z+1$.

extended polymer **1** which was slowly approached by more en step-by-step with time resulting in the formation of more open $Cu_4$ units in **2** and **3**. To the best of our knowledge, such a step-by-step structural transformation of metal−azido systems controlled by the amount of the blocking ligand was not reported earlier. The slow structural transformation of the basic $Cu_4$ basic unit from complex **1** to **3** is shown in Scheme 2.

**Magnetic Behavior. Complex 1.** The plot of $\chi_M$ versus $T$ data for **1** indicates (Figure 6 and Supporting Information) that the $\chi_M$ per $Cu^{II}_5$ unit slowly increases from 0.00879 $cm^3$ $mol^{-1}$ at 300 K with the decrease in temperature to a value of 1.14429 $cm^3$ $mol^{-1}$ at 8 K and then rapidly decreases to 0.08595 $cm^3$ $mol^{-1}$at 4 K which further increases to 0.905565 $cm^3$ $mol^{-}$upon cooling to 2 K. The product $\chi_M T$ (2.567 $cm^3$ K $mol^{-1}$) value at room temperature is slightly more than the expected value for five isolated $Cu^{II}$ions ($\chi_M T = 1.87$ $cm^3$ K $mol^{-1}$ for five $S = 1/2$ ions with $g = 2.00$). The increasing nature of the $\chi_M T$ versus $T$ plot (Figure 6) upon cooling, as well as the room temperature $\chi_M T$ value, is indicative of the presence of dominant ferromagnetic interaction in complex **1**. The room temperature $\chi_M T$ value per $Cu^{II}_5$ (2.567 $cm^3$ K $mol^{-1}$) increases rapidly to $\chi_M T = 9.35$ $cm^3$ K $mol^{-1}$ upon cooling at 8 K then decreases to $\chi_M T = 1.71$ $cm^3$ K $mol^{-1}$ at 2 K. The continuous increase of $\chi_M T$ value from room temperature down to 8 K is caused by the ferromagnetic interaction within the rail-road 1D unit, where the Cu−N−Cu angles are in the range for ferromagnetic interaction. The sharp decrease in the $\chi_M T$ value below 8 K is presumably because of the interchain interaction via the well-known end-to-end azido antiferromagnetic coupler or because of intermoleculer antiferromagnetic interaction at low temperature. The Curie−Weiss law is obeyed above 25 K with values $C = 2.328$ $cm^3$ K $mol^{-1}$ and $\theta = 41.72$ K. The positive value of Weiss constant is indicative of ferromagnetic interaction in the complex. The basic secondary building unit in this complex is a defective dicubane. Neighboring dicubanes are coupled further by end-on azido linker to form a rail-road 1D chain (Figure-1).[12] The neighboring 1D chains were linked by $Cu(en)_2^{2+}$ through the antiferromagnetic end-to-end azido coupler. The geometry around the $Cu^{II}$ ions is either square pyramidal or octahedral with axially elongated bond lengths. This indicates that the unpaired electron on each $Cu^{II}$ is residing in the basal $d_{x^2-y^2}$ orbital, while the $d_{z^2}$ orbital contains the paired electrons. Interestingly, in complex **1** the end-to-end azido links the equatorial sites (magnetic orbitals) of the $Cu^{II}$, and thus the interaction through this pathway cannot be ignored to analyze the whole magnetic data set. Thus, it is a clear case of overparameterization. To avoid the overparameterization, we have attempted to fit only the data down to 8 K (ferromagnetic region) using a defective biscubane model considering interbiscubane interaction (see Supporting Information).

The magnetic behavior of complex **1** was further characterized by field-dependent magnetization measurements at different temperatures below 20 K. As illustrated in Figure 7, the magnetization curves at 2 and 4 K clearly display a clear rise in $M$ versus $H$ at low field, and then smoothly

(12) (a) Serna, Z. E.; Lezama, L.; Urtiaga, M. K.; Arriortua, M. I.; Barandika, M. G. B.; Cortés, R.; Rojo, T. *Angew. Chem., Int. Ed.* **2000**, *39*, 344. (b) Zhang, L.; Tang, L.; Wang, Z. H.; Du, M.; Julve, M.; Lloret, F.; Wang, J. T. *Inorg. Chem.* **2001**, *40*, 3619.

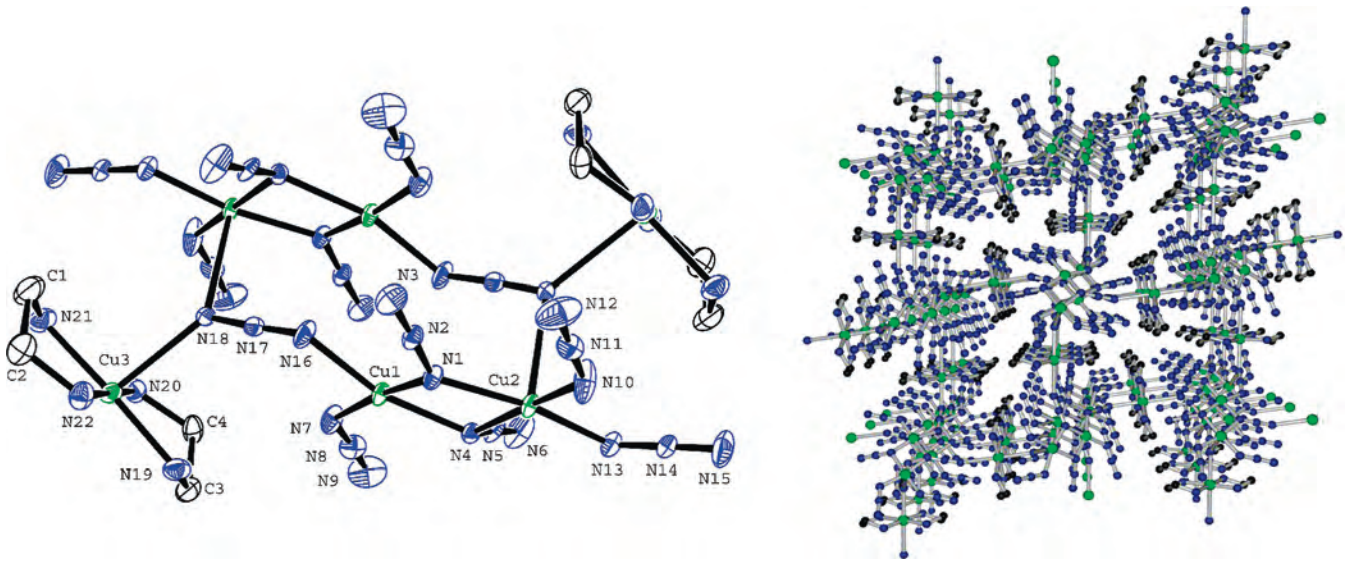


**Figure 3.** Basic secondary building unit in complex **2** (left) and the view of the complicated 3D structure (right).

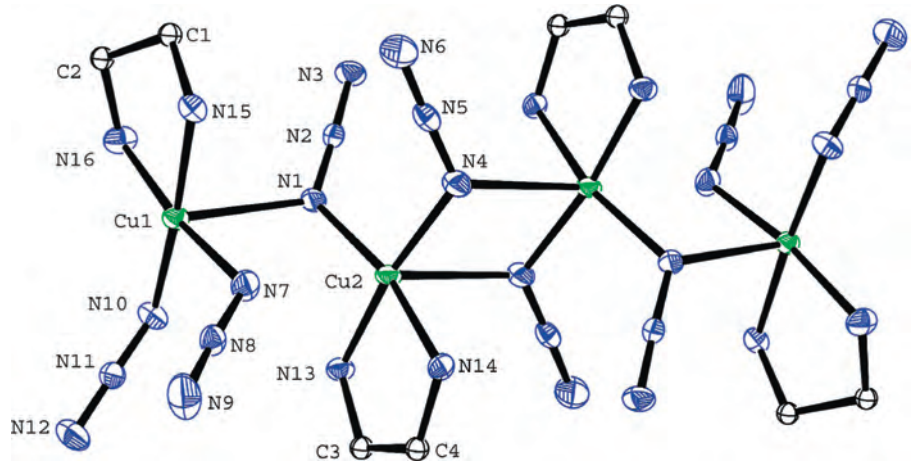


**Figure 4.** $Cu_4$ basic unit in **3** with atom-numbering scheme.

increase to the saturation magnetization ($M_s$) of about 4.45 N$\beta$ per $Cu^{II}_5$ unit at 5 T. The experimentally observed magnetization is little less than the value of 5.0 N$\beta$ anticipated for five independent $Cu^{II}$ with $S = 1/2$ ground state. The temperature dependent magnetization data in the low temperature region at different applied fields are shown in Figure 8. At low fields of 0.5, 0.7, and 0.8 T, the magnetization curves show a maximum at ~8 K, which disappears at an applied magnetic field of more than 0.8 T (1.0 and 2.0 T). This indicates an antiferromagnetic ordering at 8 K, and the external field (when the applied field is above 0.8 T) is large enough to overcome the antiferromagnetic[13] interactions to result in an ordered ferromagnetic phase below 8 K. These features are characteristic of a metamagnetic material. The sigmoidal nature of the $M$/N$\beta$ versus $H$ curve at 2 K also suggests the field-induced transition from an antiferromagnetic to a ferromagnetic state (Figure 7). These features indicate the metamagnetic nature of the complex **1**. The critical field $H_c$= 0.8 T for this metamagnetic[14] transition is approximately determined by the sharp peak of $\delta M/\delta H$ (inset of Figure 7).

The presence of weak ferromagnetism and the small magnetization at high field might be explained by possible spin canting,[14] resulting from the local magnetic anisotropy[14,15] of $Cu^{II}$ ions. For a weak ferromagnet caused by spin canting, the magnetic behavior should be quite field-dependent. As expected, the $\chi_M T$ versus $T$ shows the maximum at low temperatures and decreasing values with increasing applied field (Figure 8). From another viewpoint, the spin-canted ferromagnetism can be evidenced by the resulting magnetizations ($M-H$ plots) increasing rapidly at very low fields, whereas the magnetizations increase slowly

(13) (a) Lui, T.-F.; Sun, H.-L.; Gao, S.; Zhang, S.-W.; Lau, T.-C. *Inorg. Chem.* **2003**, *42*, 2003. (b) Li, D.-F.; Zheng, L.-m.; Wang, X.-Y.; Haung, J.; Gao, S.; Tang, W.-X. *Chem. Mater.* **2003**, *15*, 2094–2098.

(14) (a) Colacio, E.; Domı´nguez-Vera, J. M.; Ghazi, M.; Kivekaïs, R.; Lloret, F.; Moreno, J. M.; Stoeckli-Evans, H. *Chem. Commun.* **1999**, 987. (b) Hernández, M.; Lloret, F.; Ruiz-Pérez, C.; Julve, M. *Inorg. Chem.* **1998**, *37*, 4131. (c) Chen, P.-K.; Che, Y.-X.; Zheng, J.-M.; Batten, S. R. *Chem. Mater.* **2007**, *19*, 2162–2167. (d) Wang, X.-Y.; Wang, L.; Wang, Z.-M.; Su, G.; Gao, S. *Chem. Mater.* **2005**, *17*, 6369–6380.

(15) (a) Yoon, J. H.; Lim, J. H.; Choi, S. W.; Kim, H. C.; Hong, C. S. *Inorg. Chem.* **2007**, *46*, 1529. (b) Mukherjee, P. S.; Dalai, S.; Zangrando, E.; Floret, F.; Choudhuri, N. R. *Chem. Commun.* **2001**, 1444.

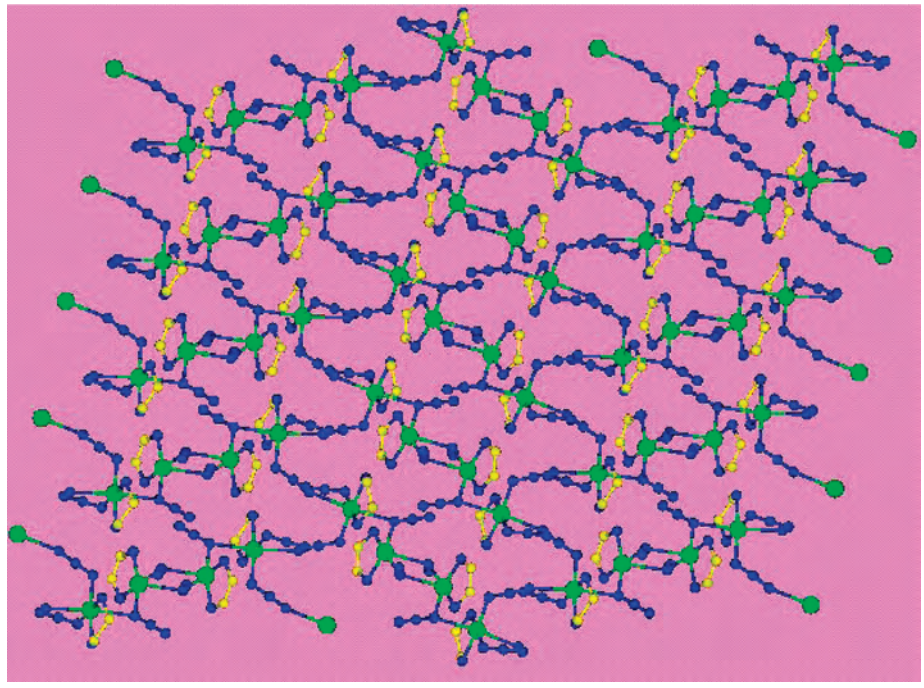

**Figure 5.** View of the 2D sheet structure of complex **3** along crystallographic *bc* plane. Color codes: blue = N, yellow = C, green = $Cu^{II}$.

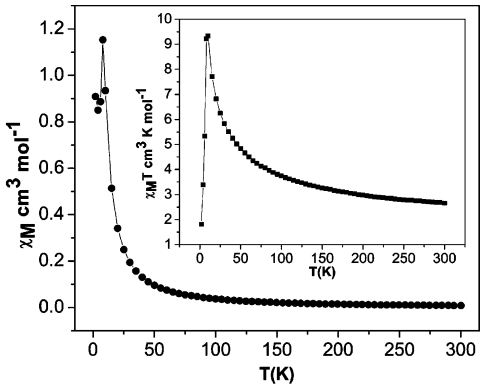


**Figure 6.** Plots of $\chi_M$ vs $T$ and $\chi_M T$ vs $T$ (inset) of complex **1** in the temperature range 2−300 K.

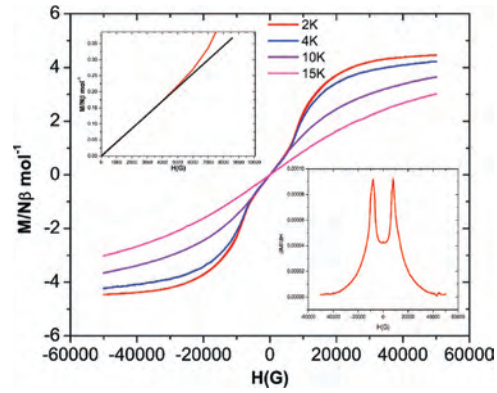


**Figure 7.** $M$ vs $H$ plots of complex **1** at the indicated temperatures.

and linearly in high-field region. Extrapolating the reversible linear part of the sigmoidal shape curve to zero field gives a magnetization value ($M_r$) of 0.26 N$\beta$ (inset Figure 7). Assuming this to be the uncompensated magnetization, the spin-canting angle[16] [$\sin \alpha = M_r/M_s$] is estimated to be about 3.34°. The magnetic phase transformation (from ferromagnetism to antiferromagnetism) was observed below 8 K.

The EPR spectrum of **1** was recorded on powdered sample at X-band between 3.9 and 13 K (Figure-9). The EPR spectra of complex **1** at different temperatures are isotropic with a $g$ value of 2.07 (3240 G), which remains unchanged with the variation in temperature. This $g$ value is characteristic

**Scheme 2.** Structural Transformation of the $Cu_4$ Cores in the Complexes **1**−**3**

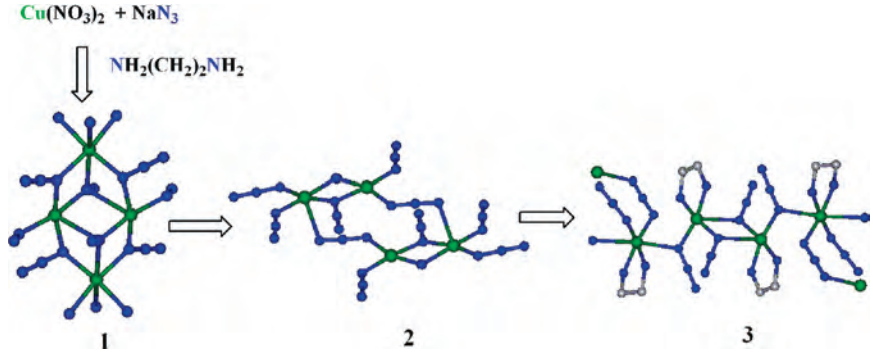

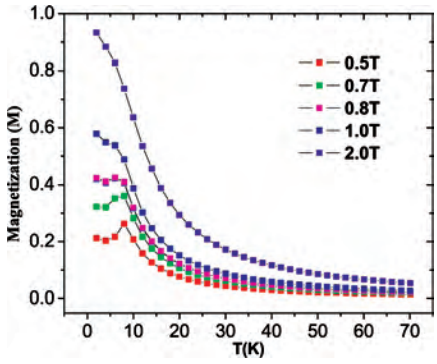


**Figure 8.** *M* vs *T* plots in the temparature range of 70−2 K for complex **1** at indicated applied magnetic fields.

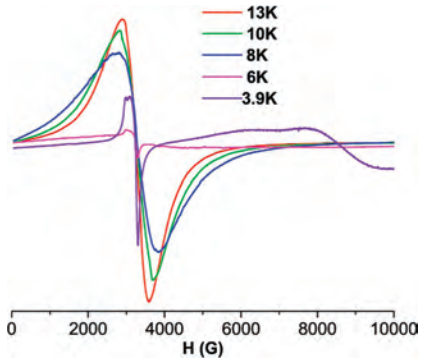


**Figure 9.** Powder X-band EPR spectra of complex **1** at different indicated temperatures.

of a $Cu^{II}$ ion.[17] The intensity of EPR spectrum decreases with the decrease in temperature from 13 to 8 K, with broadening of the line width. The line width was maximum at 8 K, presumably because of strong spin correlation,[18] and then both line width and intensity decrease at 6 K because of the long-range antiferromagnetic ordering between the ferromagnetically coupled 1D rail-road chains. The intensity of EPR signal increases and sharpens abruptly at 3.9 K with two additional features at around 7000 and 8700 G. The presence of a maximum and a minimum in the thermal evolution of the intensity and the line width can be caused by a spin canting[18b] or some kind of decompensation of the antiferromagnetically aligned spins.

**Complex 2.** The plots of both $\chi_M$ versus $T$ and $\chi_M T$ versus $T$ for **2** per $Cu^{II}_6$ unit are shown in Figure-10. The room temperature $\chi_M T$ value of 2.65 $cm^3$ K $mol^{-1}$ is slightly more than the uncoupled six $Cu^{II}$ions ($\chi_M T = 0.375$ $cm^3$ K $mol^{-1}$ for a $S = 1/2$ ion). The $\chi_M T$ value gradually increases upon decreasing temperature from room temperature and reaches a maximum value of 2.86 $cm^3$ K $mol^{-1}$ at 70 K. Further cooling decreases the $\chi_M T$ value to 1.05 $cm^3$ K $mol^{-1}$ at 2 K. The nature of the $\chi_M T$ versus $T$ plot and the room-temperature magnetic moment are the characteristics of a dominant ferromagnetic material.

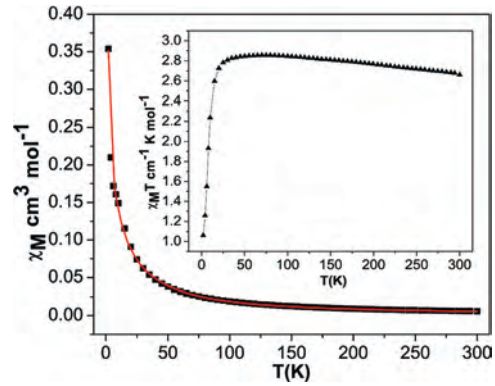


**Figure 10.** Plots of $\chi_M$ vs $T$ and $\chi_M T$ vs $T$ (inset) for complex **2** in the temperature range of 2−300 K. The red line indicates the fitting using theoretical model (see text).

**Scheme 3.** Schematic View of the Basic $Cu^{II}_4$ Magnetic Core

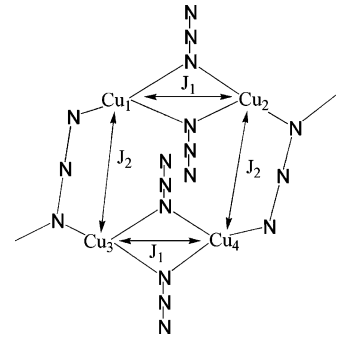


From the structural point of view, end-on azido-bridged two $Cu^{II}_2$ dimers are further linked by two longer 1,1,3-azido pathways.[19] The Cu−N−Cu angles within the $Cu^{II}_2$ dimer unit were far below the critical angle (<108°) above which systems show antiferromagnetic behavior. The basic magnetic core can be described as shown in Scheme 3. The $J_1$ corresponds to the strong interaction through the end-on azido pathway, while the $J_2$ corresponds the end-to-end azido pathway of the 1,1,3-bridging azido (Scheme 3). The spin Hamiltonian for the main magnetic unit can be written as $H = -J_1(S_1S_2 + S_3S_4) - J_2(S_1S_3 + S_2S_4)$, where $S_1 = S_2 = S_3 = S_4 = 1/2$. Considering these two different exchange parameters values, the analysis of the experimental susceptibility values has been performed using the following expression:

$$\chi_M = [Ng^2\beta^2/kT][A/B] \quad (1)$$

where $A = [30\exp(-E_1/kT) + 6\exp(-E_2/kT) + 6\exp(-E_3/kT) + 6\exp(-E_4/kT)]$, $B = 5[\exp(-E_1/kT) + 3\exp(-E_2/kT) + 3\exp(-E_3/kT) + 3\exp(-E_4/kT) + \exp(-E_5/kT) + \exp(-E_6/kT)]$. The $E_{1-6}$ values were obtained from the above Hamiltonian using Kambe method: $E_1 = -(J_1 + J_2)/2$, $E_2 = (J_2 - J_1)/2$, $E_3 = (J_1 + J_2)/2$, $E_4 = (J_1 - J_2)/2$, $E_5 = (J_1^2 + J_2^2 - J_1J_2)^{1/2} + (J_1 + J_2)/2$, and $E_6 = (J_1 + J_2)/2 - (J_1^2 + J_2^2 - J_1J_2)^{1/2}$. The best-fit parameters obtained are $J_1 =$

(16) Bellitto, C.; Federici, F.; Colapietro, M.; Portalone, G.; Caschera, D. *Inorg. Chem.* **2002**, *41*, 709.
(17) Bencini, A.; Gatteschi, D. *EPR of Exchange Coupled Systems*; Springer-Verlag: Berlin, 1990.
(18) (a) Bazan, B.; Mesa, J. L.; Pizarro, J. L.; Fernandez, J. R.; Marcos, J. S.; Roig, A.; Molins, E.; Arriortua, M. I.; Rojo, T. *Chem. Mater.* **2004**, *16*, 5249. (b) Chung, U.-C.; Mesa, J. L.; Pizarro, J. L.; Fernandez, J. R.; Marcos, J. S.; Gartaonandia, S. S.; Arriortua, M. I.; Rojo, T. *Inorg. Chem.* **2006**, *45*, 8965.
(19) Ray, U.; Sarkar, K. K.; Mostafa, G.; Lu, T. H.; El Fallah, M. S.; Sinha, C. *Polyhedron* **2006**, *25*, 2764.

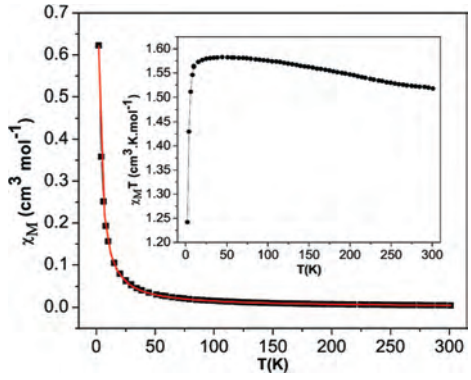


**Figure 11.** Plots of $\chi_M$ vs $T$ and $\chi_M T$ vs $T$ (inset) of complex **3** in the temperature range of 2−300 K. The red line indicates the fitting.

$+ 208.02\ cm^{-1}$, $J_2 = -4.89\ cm^{-1}$, $g = 2.03$, and $R = 3.0 \times 10^{-4}$.

The end-on azido pathway within the Cu−$(N_3)_2$−Cu dimer mediates the strong ferromagnetic interaction. Such strong ferromagnetic interactions were found in several end-on azido bridged $Cu^{II}$ dimers with analogous structural parameters.[20a,b] The azido nitrogens link through the equatorial $d_{x^2-y^2}$ magnetic orbitals, and thus the magnetic interaction through this pathway is strong. On the other hand, the antiferromagnetic interaction mediates through the end-to-end pathway of the 1,1,3-azido moieties. In this case, one terminal nitrogen of the azido links the equatorial site of one $Cu^{II}$, while the other end nitrogen links the nonmagnetic axial site ($d_{z^2}$) of the other $Cu^{II}$, which results in a low exchange parameter.

**Complex 3.** The $\chi_M T$ value (0.3795 $cm^3\ K\ mol^{-1}$) at room temperature is very close to the expected value for an isolated $Cu^{II}$ of spin $S = 1/2$ ($\chi_M T = 0.375\ cm^3\ K\ mol^{-1}$). The increasing nature of the $\chi_M T$ vs $T$ plot (Figure 11) down to 44 K is an indication of the existence of ferromagnetic interaction. The $\chi_M T$ value at 44 K is 0.39577 $cm^3\ K\ mol^{-1}$, which decreases further very quickly upon cooling and reaches a value of 0.3107 $cm^3\ K\ mol^{-1}$ at 2 K, which indicates that in the temperature range of 300−44 K ferromagnetic interactions dominates over antiferromagnetic interaction and below 44 K the reverse order is followed. The basic repeating unit in the complex is a $Cu_4$ linear unit where two single EO azido-bridged $Cu_2$ dimers are further linked by double EO azido linker. Thus our initial attempt was to fit the magnetic susceptibility data using a dimeric model of $Cu^{II}$ considering the interdimer interaction. The best fitting parameters were $J_1 = 4.02\ cm^{-1}$, $J_2 = -1.2\ cm^{-1}$, and $R = 2.7 \times 10^{-4}$ when $g = 2.01$. However, in this case, the fitting was not satisfactory. To improve the fitting quality, we considered the following model of a $Cu_4$ with two different $J$ values.

The basic core can be described as Cu(1)−$J_1$−Cu(2)−$J_2$−Cu(3)−$J_1$−Cu(4), and because the central $Cu^{II}$ ions are bridged by double EO azido, $J_1$ and $J_2$ will not be identical.[21] The spin Hamiltonian for this discrete $Cu_4$can be described as $H = -J_1(S_1S_2 + S_3S_4) - J_2S_2S_3$.The equation giving the temperature dependence of susceptibility per $Cu^{II}$ of this cluster obtained was

$$\chi_M^{\text{cluster}} = \frac{Ng^2\beta^2 A}{12k_B T B} \tag{2}$$

where

$$A = 30\exp\left(\frac{\frac{J_1}{2}+\frac{J_2}{4}}{kT}\right) + 6\exp\left(\frac{-\frac{J_1}{2}+\frac{J_2}{4}}{kT}\right) + 6\exp\left(\frac{-\frac{J_2}{4}-\frac{\sqrt{J_1^2+J_2^2}}{2}}{kT}\right) + 6\exp\left(\frac{-\frac{J_2}{4}+\frac{\sqrt{J_1^2+J_2^2}}{2}}{kT}\right)$$

$$B = 5\exp\left(\frac{\frac{J_1}{2}+\frac{J_2}{4}}{kT}\right) + 3\exp\left(\frac{-\frac{J_1}{2}+\frac{J_2}{4}}{kT}\right) + 3\exp\left(\frac{-\frac{J_2}{4}-\frac{\sqrt{J_1^2+J_2^2}}{2}}{kT}\right) + 3\exp\left(\frac{-\frac{J_2}{4}+\frac{\sqrt{J_1^2+J_2^2}}{2}}{kT}\right) + \exp\left(\frac{-\frac{J_1}{2}-\frac{J_2}{4}-\frac{\sqrt{4J_1^2-2J_1J_2+J_2^2}}{2}}{kT}\right) + \exp\left(\frac{-\frac{J_1}{2}-\frac{J_2}{4}+\frac{\sqrt{4J_1^2-2J_1J_2+J_2^2}}{2}}{kT}\right)$$

The linear $Cu_4$ cluster units in the 2D polymer of **3** are linked further by cis-EE azido linker, and thus the intercluster interaction (eq 3) was considered to fit the susceptibility data of this complex.

$$\chi_M^{\text{intercluster}} = \frac{1}{\frac{1}{\chi_M^{\text{cluster}}} - \frac{2ZJ'}{Ng^2\beta^2}} \tag{3}$$

The nature of fitting and $R$ factor both were improved, and the best-fit parameters are $J_1 = 1.29\ cm^{-1}$, $J' = -0.75996\ cm^{-1}$, and $J_2 = +2.32\ cm^{-1}$ at $g = 2.01$ with $R = 1.8 \times 10^{-7}$.

Two peripheral $Cu^{II}$ ions of the linear $Cu_4$ basic units are in octahedral environment, whereas the other two middle $Cu^{II}$ are in square-pyramidal geometries. The longer axial bond lengths in both the cases indicate the presence of unpaired electron in the basal $d_{x^2-y^2}$ orbital. The Cu−N−Cu bond angles for both the pathways are less than 108° and are thus expected to mediate ferromagnetic interactions through these pathways. The weak exchange interaction through both these pathways are the result of the axial−equatorial bridging fashion. The intercluster antiferromagnetic interaction mediates through the cis-EE pathway.

(20) (a) Escuer, A.; Goher, M. A. S.; Mautner, F. A.; Vicente, R. *Inorg. Chem.* **2000**, *39*, 2107. (b) Sikorav, S.; Bkouche-Waksman, I.; Kahn, O. *Inorg. Chem.* **1984**, *23*, 490. (c) Munno, G. D.; Lombardi, M. G.; Julve, M.; Lloret, F.; Faus, J. *Inorg. Chim. Acta* **1998**, *282*, 82. (d) Costes, J. P.; Dahan, F.; Ruiz, J.; Laurent, J. P. *Inorg. Chim. Acta* **1995**, *239*, 53. (e) Li, L.; Liao, D.; Jiang, Z.; Yan, S. *Polyhedron* **2001**, *20*, 681.

(21) Madalan, A. M.; Noltemeyer, M.; Neculai, M.; Roesky, H. W.; Schimdtmann, M.; Muller, A.; Journaux, Y.; Andruh, M. *Inorg. Chim. Acta* **2006**, *359*, 459.

## Concluding Remarks

In summary, three new Cu−azido polymers have been synthesized by changing the amount of the blocking diamine ligand (en) in a systematic way. All the three complexes are fully characterized by X-ray structure determination and variable-temperature magnetic behavior down to 2 K. Complexes **1** and **2** are 3D polymers containing incomplete $Cu_4$ double-cubane and relatively open $Cu_4$ macrocyclic repeating units, respectively. The gradual change in the $Cu_4$ basic units in the complexes upon addition of more and more en ligand was clearly observed from X-ray analysis. The more close and puckered $Cu_4$ unit was opened up in a stepwise manner when more and more en approached to the $Cu_4$ moiety to result a more open linear $Cu_4$ unit with one en per Cu in complex **3**. Complex **1** represents the first example of metal-azido system containing four different bridging modes of azido. Complex **3** contains two very rare cis-EE and single-EO azido modes. Interestingly, the Cu−N−Cu bond angle through the single EO pathway is smaller than that through the double EO pathway although the reverse order is expected. The magnetic behavior of complex **1** was very interesting with a dominant ferromagnetic nature and an antiferromagnetic order at low temperature. *M* versus *H* plots at different low temperatures, as well as *M* versus *T* plots at different external magnetic field, established the metamagnetic like behavior with a critical field of 0.8 T. Complex **2** was a strong ferromagnetic, and the last one was a dominant weak ferromagnetic. Magnetic data were fitted reasonably well using several theoretical models. It has been well established that a simple change to the substitution on the blocking amine changes the bridging mode of azido and the gross structures of metal−azido systems. Moreover, the role of the amount of azido and reaction condition on the diversity of metal−azido systems have been well established. The amount of blocking amine should in principle change the nuclearity and the gross structure of azido−metal system. Our present results represent a report on the systematic change in the structure/dimensionality and magnetic properties of Cu−azido polymers controlled by the amount of blocking amine ligand. The change in the amount of blocking amine ligand in conjunction with metal−azido systems and formation of variety of assemblies has the potential to considerably expand this methodology.

**Acknowledgment.** The authors acknowledge the Department of Science and Technology, New Delhi, and CSIR, New Delhi, Government of India, for financial support to P.S.M. The authors sincerely thank all the reviewers for their evaluations and very fruitful suggestions. The authors also appreciate the help from Sandip Ghosh on the powder XRD data collection and Debmalya Bannerjee and Prof. S. B. Bhat for their help on EPR measurements.

**Supporting Information Available:** X-ray crystallographic file in CIF format, fitting of magnetic data in the range of 300−8 K for **1**, and powder XRD patterns of the complexes **1**−**3**. This material is available free of charge via the Internet at http://pubs.acs.org.

IC702232D